Progress of Theoretical Physics, Vol. 71, No. 2, February 1984

Fates of Three-Torus. I

—— *Double Devil's Staircase in Lockings* ——

Kunihiko KANEKO

Department of Physics, University of Tokyo, Tokyo 113

(Received July 13, 1983)

Fates of three-torus are investigated by two- or four-dimensional coupled mappings. Three-tori exist for a weak coupling, which become feasible to lock into a torus as the coupling increases. Transition to chaos occurs only via a locking into a cycle. The locking into a torus forms a "double devil's staircase", which is studied by the modulated circle map. Mechanism of the locking is also discussed.

§ 1. Introduction

In recent years, transition from a torus to chaos has been extensively studied.[1)~21)] The phase motion of torus is investigated using a one-dimensional mapping[3)~6),10)~12)]

$$\theta_{n+1}=\theta_n+A\sin(2\pi\theta_n)+D\,, \tag{1·1}$$

where various scaling properties of the locking state are found and renormalization group approach[8),9)] based on Feigenbaum's theory has been executed. The amplitude motion of torus is also studied with the use of two- or three- dimensional mapping, where the distortion of torus and doubling of torus are discovered[13),14)] and their mechanisms are clarified.[15)] The intermittency of torus has also been studied.[16)] These results of mappings are also confirmed in flow systems.[17)~19)]

There remains, however, a fundamental problem, that is, a transition from three-torus*) to chaos. Three-tori appear via a Hopf bifurcation of a torus. In 1971, Ruelle and Takens pointed out the structural instability of a three-torus and the emergence of a strange attractor.[1),2)] In experiments, however, three-tori have seemed to be observed,[19),20)] but it is not so clear whether the attractor is three-torus or two-torus in the experiments. Numerical studies on a three-torus, however, are very few except the simulation of a 56-mode truncation of the Navier-Stokes equation by Yahata.[21)] Thus, it will be of importance to study the features of a three-torus in a simple system.

The successive Hopf bifurcations can be modeled by the equations

$$\dot{w}_j=(\gamma_0-d(j))w_j-(g_1+ig_2)|w_j|^2w_j+\varepsilon h_j(w_1,\ w_1^*,\ w_2,\ w_2^*,\ \cdots,\ w_N,\ w_N^*), \tag{1·2}$$

$$(j=1,\ 2,\ \cdots,\ N)$$

where γ_0 is a bifurcation parameter and w is a complex order parameter. When ε is zero, successive Hopf bifurcations occur at $\gamma_0=d(i)$ and a k-torus appears (k is a number of j which satisfies $\gamma_0>d(j)$). As the perturbation εh sets in, the direct product state may become unstable, and the k-torus can be destroyed. Though it will be of interest to study

*) In the present paper, the terminology "three-torus" means the quasiperiodic motion with three incommensurate frequencies, while the terminology "torus" (or two-torus) means the one with two incommensurate frequencies.

Eq. (1·2), we make a further simplification in the present paper, that is, we make use of a coupled map.

Since the dimensionality is reduced by one by taking a Poincaré map from a flow system, the three-torus in a flow corresponds to an attractor in a map with the first and second Lyapunov exponents vanishing. Thus, we choose the following mapping as a model of a three-torus:

$$\begin{cases} x_{n+1}=f(x_n, y_n; a)+\varepsilon h_1(x_n, y_n, z_n, w_n), \\ y_{n+1}=g(x_n, y_n; a)+\varepsilon h_2(x_n, y_n, z_n, w_n), \\ z_{n+1}=f(z_n, w_n; a')+\varepsilon h_3(x_n, y_n, z_n, w_n), \\ w_{n+1}=g(z_n, w_n; a')+\varepsilon h_4(x_n, y_n, z_n, w_n), \end{cases} \tag{1·3}$$

where the mappings $x_{n+1}=f(x_n, y_n; a)$, $y_{n+1}=g(x_n, y_n; a)$ show the transition from torus to chaos as the bifurcation parameter a is increased, and $\varepsilon h_i (i=1, 2, 3, 4)$ are perturbations. In §2, we take the delayed logistic model (see Appendix and Ref. 13)) for $\{f, g\}$, to study the stability of a three-torus.

If our interest is restricted only to the phase motion of the three-torus, a further simplification may be possible just as in the study of two-torus by map (1·1). Thus, a coupled circle map

$$\begin{cases} \theta_{n+1}=\theta_n+A\sin(2\pi\theta_n)+D+\varepsilon\sin(2\pi\varphi_n), \\ \varphi_{n+1}=\varphi_n+B\sin(2\pi\varphi_n)+C+\varepsilon'\sin(2\pi\theta_n) \end{cases} \tag{1·4}$$

will be of relevance to the study of the phase motion of a three-torus. In §3, the simplest case among mappings (1·4) is investigated, that is the "modulated circle map". Various lockings into torus are found. The winding number as a function of a bifurcation parameter forms a "double devil's staircase", which will also be shown in §3.

The main purpose of the present paper is to give only qualitative features of a three-torus with various figures. In this sense, the understanding of three-torus remains rather incomplete. Discussion including the unresolved problems will be given in §4.

§ 2. Three-torus in a 4-dimensional mapping

In this section, we show numerical results on the 'coupled delayed logistic map', to discuss the stability of three-torus. Delayed-logistic map is given by

$$x_{n+1}=Ax_n+Dx_{n-1}(1-x_{n-1}), \tag{2·1}$$

which shows a transition "fixed point →(Hopf bifurcation)→ torus → locking →chaos→hyperchaos" as D is increased (see also the Appendix for the properties of a delayed map). According to the idea in §1, we couple two delayed-logistic mappings and add a perturbation. The model equations, constructed in this way, are

$$\begin{cases} x_{n+1}=Ax_n+D_1x_{n-1}(1-x_{n-1})+\varepsilon h_1(x_n, x_{n-1}, z_n, z_{n-1}), \\ z_{n+1}=Az_n+D_2z_{n-1}(1-z_{n-1})+\varepsilon h_2(x_n, x_{n-1}, z_n, z_{n-1}). \end{cases} \tag{2·2}$$

Equation (2·2) is a 4-dimensional map $(x_n, y_n, z_n, w_n)\to(x_{n+1}, y_{n+1}, z_{n+1}, w_{n+1})$, where $y_n\equiv x_{n-1}$ and $w_n\equiv z_{n-1}$. In the present paper the value A is fixed at 0.4, though the

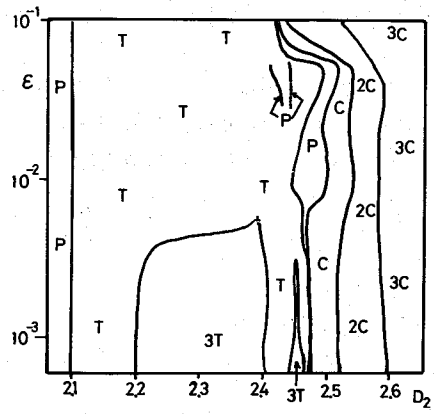

Fig. 1. Phase diagram of map (2·2) with $D_1=D_2+0.1, h_1=z_n-z_{n-1}$ and $h_2=x_{n-1}-x_n$. The notations P, T, $3T$, C and nC denote periodic state (cycle), torus, 3-torus, chaos and hyperchaos with n positive Lyapunov exponents.

qualitative behaviors are insensitive to the change of A. As is given in the Appendix, the delayed logistic map shows a Hopf bifurcation at $D=D_c=3-2A=2.2$ and a torus appears for $D>D_c$, which is destroyed via lockings and chaos appears for $D\gtrsim 2.59$. Thus, the direct product state, such as $T\otimes P$, $T\otimes T$, $C\otimes T$, $C\otimes C$ (P, T, and C denote periodic state (cycle), torus, and chaos respectively) exists correspondingly to the values D_1 and D_2, for $\varepsilon=0$.

As the perturbations set in, the direct product state can become unstable. Here, we chose the perturbations as $h_1=z_n-z_{n-1}$ and $h_2=x_{n-1}-x_n$ and made simulations of map (2·2) for various values of D_1, D_2 and ε, to study the stability of the direct product

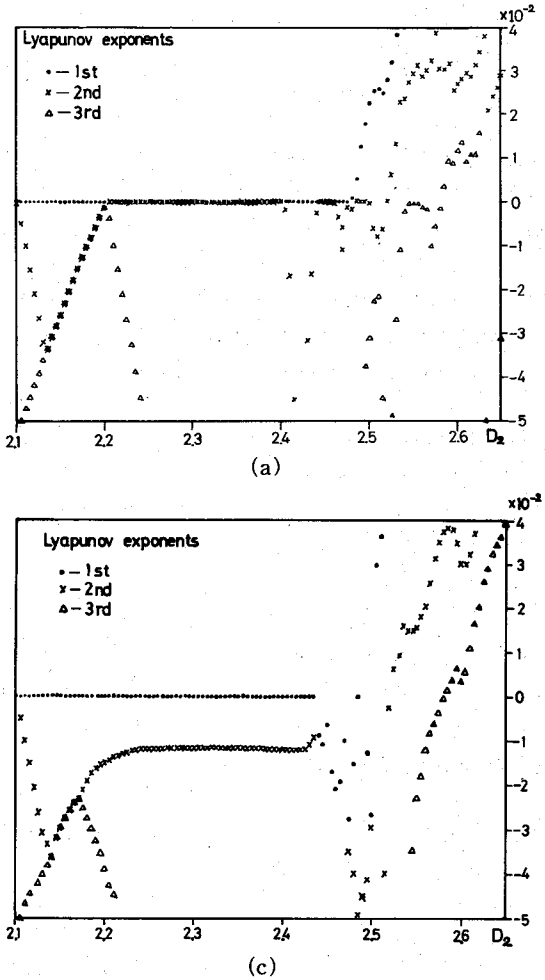

Fig. 2. Lyapunov exponents for map (2·2) with $D_1=D_2+0.1$, $h_1=z_n-z_{n-1}$ and $h_2=x_{n-1}-x_n$, which were calculated by the method due to Shimada and Nagashima.[23] The values of ε are 10^{-3}(a), 5×10^{-3}(b) and 10^{-2}(c) respectively. The first (●), second (×), and third (△) Lyapunov exponents are plotted for $2.1\leq D_2\leq 2.65$, while the fourth exponent is large in magnitude (negative) and is omitted.

state.

In Fig. 1, a rough phase diagram for the map is given, where the parameter D_1 is taken as $D_1=D_2+0.1$. We classify the attractors into cycle (P), torus (T), 3-torus ($3T$), chaos and hyper^k-chaos (kC),[22] by calculating the Lyapunov exponents from the first to the fourth.[23] Examples of Lyapunov exponents as a function of D_2 for $\varepsilon=10^{-3}$, 5×10^{-3} and 10^{-2} are given in Figs. 2(a)~(c), while examples of the attractors for $\varepsilon=5\times10^{-3}$ are shown in Figs. 3(a)~(f), where the projections onto the (x_n, z_n)-plane are depicted. In the rest of this section, we describe what is learned from these figures and other numerical results of map (2·2).

As is seen in these figures, there exists a three-torus for a small coupling ε. As the coupling increases, the region of three-torus decreases and it vanishes for $\varepsilon\gtrsim9\times10^{-3}$.

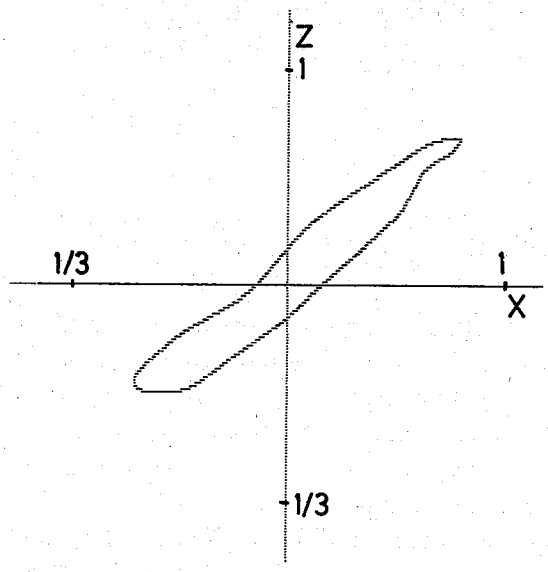

(a)

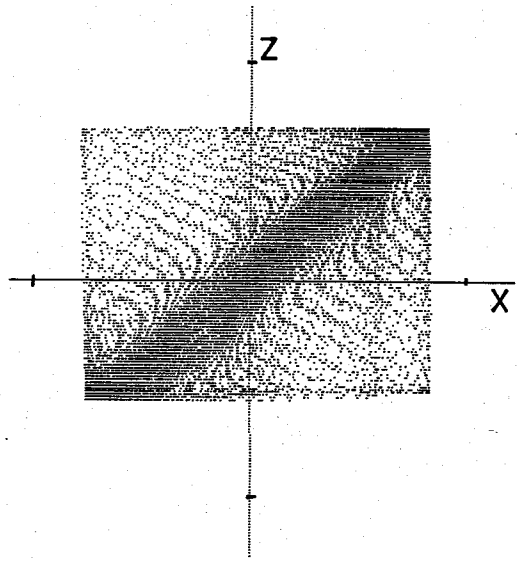

(b)

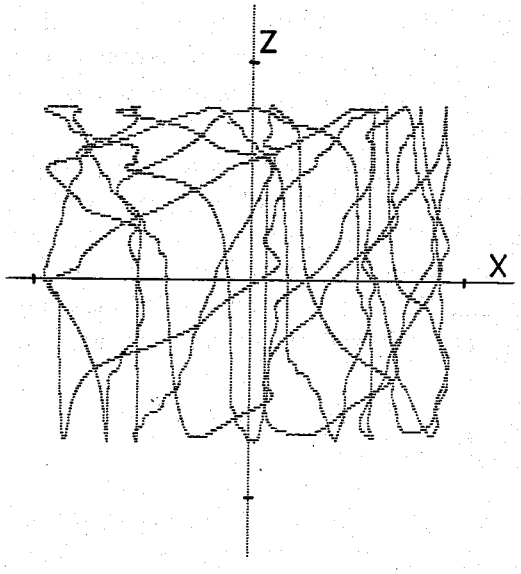

(c)

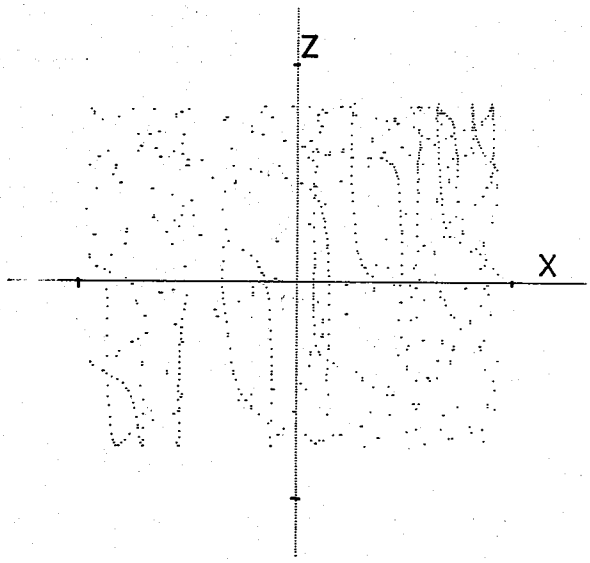

(d)

(continued)

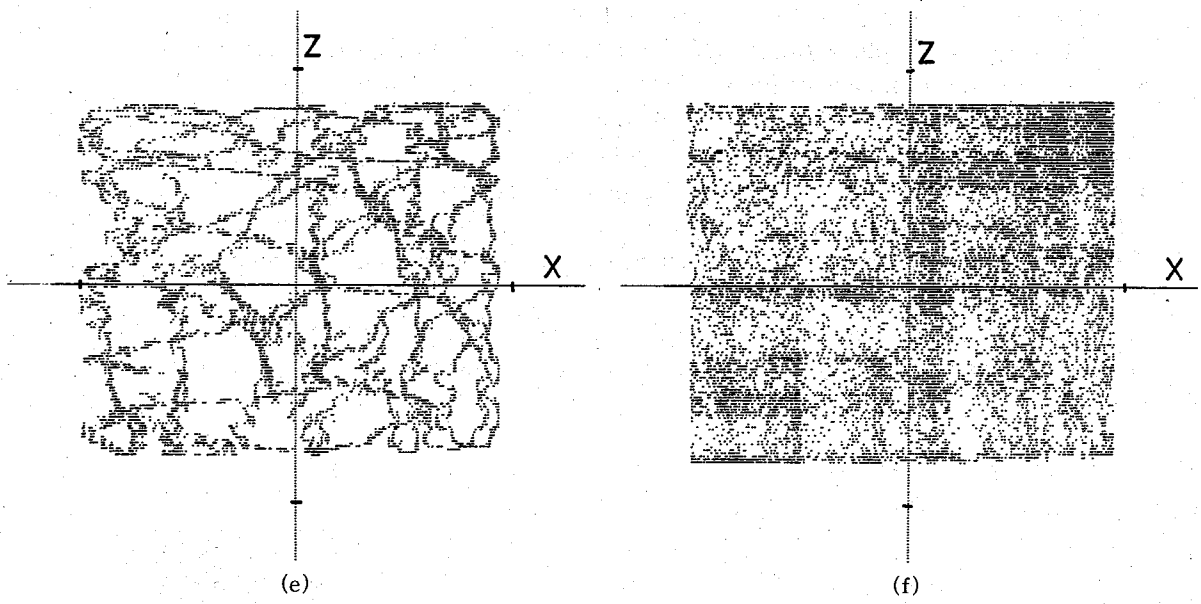

(e) (f)

Fig. 3. Projection onto the (x_n, z_n) plane of the attractor of map (2·2) with $D_1=D_2+0.1$, $h_1=z_n-z_{n-1}$ and $h_2=x_{n-1}-x_n$. The parameter ε is fixed at 5×10^{-3} and the values of D_2 are 2.35(a), 2.37(b), 2.45(c), 2.46(d), 2.47(e) and 2.48(f), respectively.

Thus, the three-torus loses its stability as the coupling increases. The attractor that emerges through this instability is not a chaos[1] but a torus. We note that the chaos appears only via a cycle which has appeared as a locking of a torus, which again appeared as a locking of a three-torus. This fact is an extension of the recent observation that the transition from torus to chaos occurs only via a locking into cycle for the circle map (1·1)[7),11),12)] (i.e., in the case that the instability in phase dynamics is relevant).

Let us see the cases of $\varepsilon=10^{-3}$, 5×10^{-3} and 10^{-2} in more detail. For $\varepsilon=10^{-3}$, the second Hopf bifurcation occurs at $D_2=D_c=2.2$ (see Fig. 2(a) and note that the 2nd and 3rd Lyapunov exponents are degenerate for $2.13\lesssim D_2\lesssim2.2$) and a three-torus appears. As the nonlinearity D_2 is increased, the region of the locking into torus increases. The locking into torus occurs wia a tangent bifurcation, which is the same for the locking into cycle.[5)] The appearance of chaos occurs at $D_2\simeq2.48$, the mechanism of which is the same for $\varepsilon=5\times10^{-3}$, which will be discussed in detail.

For $\varepsilon=5\times10^{-3}$, the second and third Lyapunov exponents are degenerate for $2.14\lesssim D_2\lesssim2.18$, but they are split before $D_2=2.2$, and the second Hopf bifurcation does not occur (see Fig. 2(b)). The attractor at $D_2=2.35$ is given in Fig. 3(a), which is regarded as a locking from a three-torus. This locking disappears via a tangent bifurcation and a three-torus appears (see Fig. 3(b)). As we increase D_2 further, various lockings into torus appear (see Fig. 3(c)). These lockings are characterized by the rotation numbers ρ_x and ρ_z, which are defined by

$$\lim_{n\to\infty}\frac{1}{2\pi n}\sum_{i=1}^{n}\arg(\overrightarrow{P_iP_{i+1}},\ \overrightarrow{P_{i+1}P_{i+2}}),$$

where $P_i=(x_i, x_{i-1})$ or (z_i, z_{i-1}) respectively. The locking in Fig. 3(a) is characterized by $\rho_x=\rho_z$. The bahaviors of lockings with rotation numbers are investigated in detail in §3 for a simplified model. For $D_2\gtrsim2.458$, the chaos appears (Fig. 3(e)) via a locking into

a cycle (Fig. 3(d)). As D_2 is increased further, the second and third Lyapunov exponents become positive successively. We note that the picture of a "direct product state" is recovered (see e.g. Fig. 3(f)) as the Lyapunov exponents get large.

For $\varepsilon=10^{-2}$, the region of the locking into a torus increases, and the three-torus has disappeared (see Fig. 2(c)). Transition from torus to chaos via lockings into cycle occurs for $D_2\simeq 2.50$, just as in the case for two-dimensional mappings.

Numerical simulations on other cases, such as $D_2=D_1$ or $\varepsilon<0$ were also performed. For $D_2=D_1$, the locking into the torus with $\rho_x=\rho_z$ is more dominant and the three-torus is not observed for $\varepsilon\gtrsim 10^{-3}$. For the case with $\varepsilon<0$ or with another type of perturbations (such as $h_1=z_n-x_n$, $h_2=x_n-z_n$), the qualitative feature is the same as the above case.

Thus, the three-torus exists for a small coupling, which becomes feasible to lock into torus as the coupling is increased and is collapsed above some "critical" coupling.

§ 3. Double devil's staircase in modulated circle map

In this section we study the phase motion of a three-torus with the use of a coupled circle map given in Eq. (1·4). Here, the simplest case $B=\varepsilon'=0$ is treated, that is, the "modulated circle map",

$$\begin{cases} \theta_{n+1}=\theta_n+A\sin(2\pi\theta_n)+D+\varepsilon\sin(2\pi\varphi_n), \\ \varphi_{n+1}=\varphi_n+C\,. \end{cases} \tag{3·1}$$

The parameter C is chosen to be irrational, which is fixed at $(\sqrt{5}-1)/2$, i.e., the inverse

Table I. Lockings of the modulated circle map with $C=(\sqrt{5}-1)/2$ and $A=0.15$. The values q/p and s/r where $\rho_\theta=q/p+C\cdot s/r$ are written. If the values are not listed, the locking with simple integers q, p, s, r does not occur. For Table I(a), ε is 0.01 and D is changed from 0.606 to 0.619 by 0.001. The value of ε is 0.1 for the other tables, where D is changed from 0.58 to 0.69 by 0.005 for I(b) and it is changed from 0.6355 to 0.6395 by 0.0005 for I(c).

(a)

D	q/p	s/r
0.606	0	1
≈	≈	≈
0.610	0	1
0.611	5/18	−5/9
0.612	5/11	3/11
0.613	5/9	1/11
0.614	5/7	1/7
0.615	5/6	−1/3
0.616	5/6	−1/3
0.617	5/6	−1/3
0.618	—	—
0.619	1/2	3/14

(b)

D	q/p	s/r
0.580	0	1
≈	≈	≈
0.630	0	1
0.635	1/5	7/10
0.640	5/2	−3
0.645	1/2	1/4
0.650	3/5	1/10
0.655	2/3	0
0.660	2/3	0
0.665	—	0
0.670	1	−1/2
≈	≈	≈
0.685	1	−1/2
0.690	—	—

(c)

D	q/p	s/r
0.6355	−4	15/2
0.6360	5/3	−5/3
0.6365	5/3	−5/3
0.6370	5/3	−5/3
0.6375	—	—
0.6380	−3/4	9/4
0.6385	−3/4	9/4
0.6390	−16/3	29/3
0.6395	−11/5	23/5

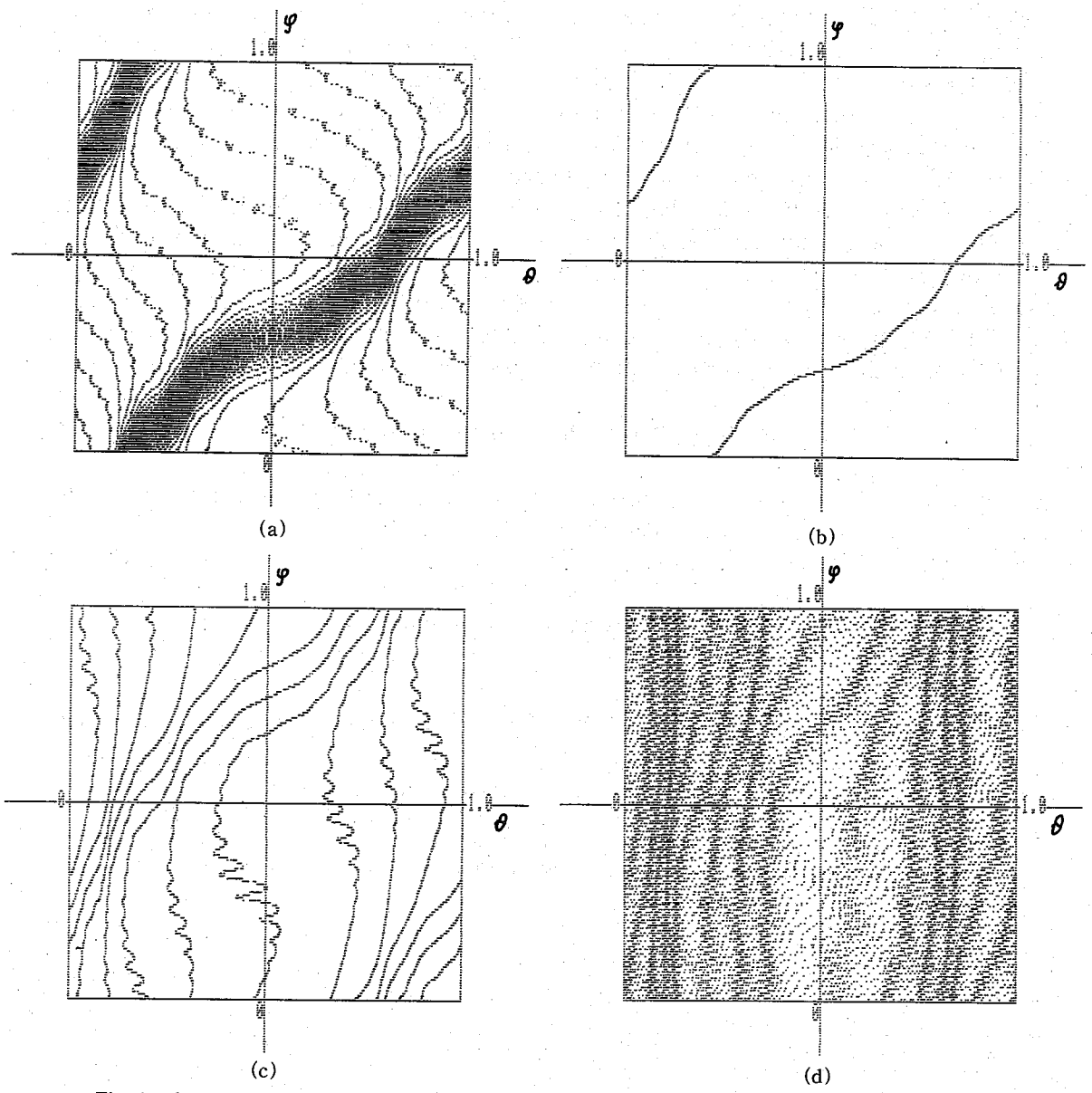

Fig. 4. Attractor of the modulated circle map (3·1) with $C=(\sqrt{5}-1)/2$, $A=0.15$ and $\varepsilon=0.01$. The points (θ_i, φ_i) $(5000\leq i\leq 25000)$ with the initial values $(\theta_0, \varphi_0)=(0.5, 0.5)$ are plotted. The values of D are 0.6052(a), 0.6055(b), 0.612(c) and 0.62(d), respectively.

of the golden mean.

One of the Lyapunov exponents is always zero and if the other is also zero, then the attractor is a three-torus (to be precise, it is the phase part of the Poincaré map of a three-torus, but we call it three-torus for simplicity in the present paper).

Map (3·1) is invertible for $A<1/(2\pi)$. The attractor for $A<1/(2\pi)$ is a torus or a three-torus, which is understood as follows: First, we approximate C by F_{n-1}/F_n using the continued fraction expansion[24] (for the case $C=(\sqrt{5}-1)/2$, F_n is a Fibonacci sequence). Iterating map (3·1) F_n times, we obtain a one-dimensional map, which is an invertible circle map and its attractor is a cycle or torus.[24] Taking a limit $n\to\infty$, we can confirm

the above statement.

The rotation number for φ is fixed at C and the rotation number ρ_θ for θ is a monotone (in a wide sense) function of D. We conjecture that for $A<1/2\pi$, the locking from three-torus into torus occurs if and only if ρ_θ takes a value $q/p+Cs/r$ (p, q and r, s are relatively prime integers respectively). The above conjecture is a natural extension of the theorem on the locking of the torus[24] and seems to hold in numerical results. In our case, we note that q or s can take a negative value even if ρ_θ is positive.

Examples of the attractors are given in Figs. 4(a)~(d) ($\varepsilon=10^{-2}$). The locking with $\rho_\theta=C$ occurs for $D\gtrsim 0.6054$ (Fig. 4(b)). As is seen in Fig. 4(a), a kind of "intermittent" behavior is seen for just a smaller value of D than 0.6054, which is typical for the tangent bifurcation[4] (see also Fig. 3(b)).

Locking with $\rho_\theta=5/11+3C/11$ is given in Fig. 4(c), while the attractor of three-torus is shown in Fig. 4(b). The values p, q, r, s (where $\rho_\theta=q/p+Cs/r$) are given in Tables I(a) ($\varepsilon=10^{-2}$), (b) and (c) ($\varepsilon=10^{-1}$). We note that the various lockings with $\rho_\theta=q/p+Cs/r$ form rather complicated structures. The rotation number ρ_θ as a function of D is given in Figs. 5(a) ($\varepsilon=10^{-3}$), (b) ($\varepsilon=10^{-2}$) and (c) ($\varepsilon=10^{-1}$). As is seen in Fig. 5 and

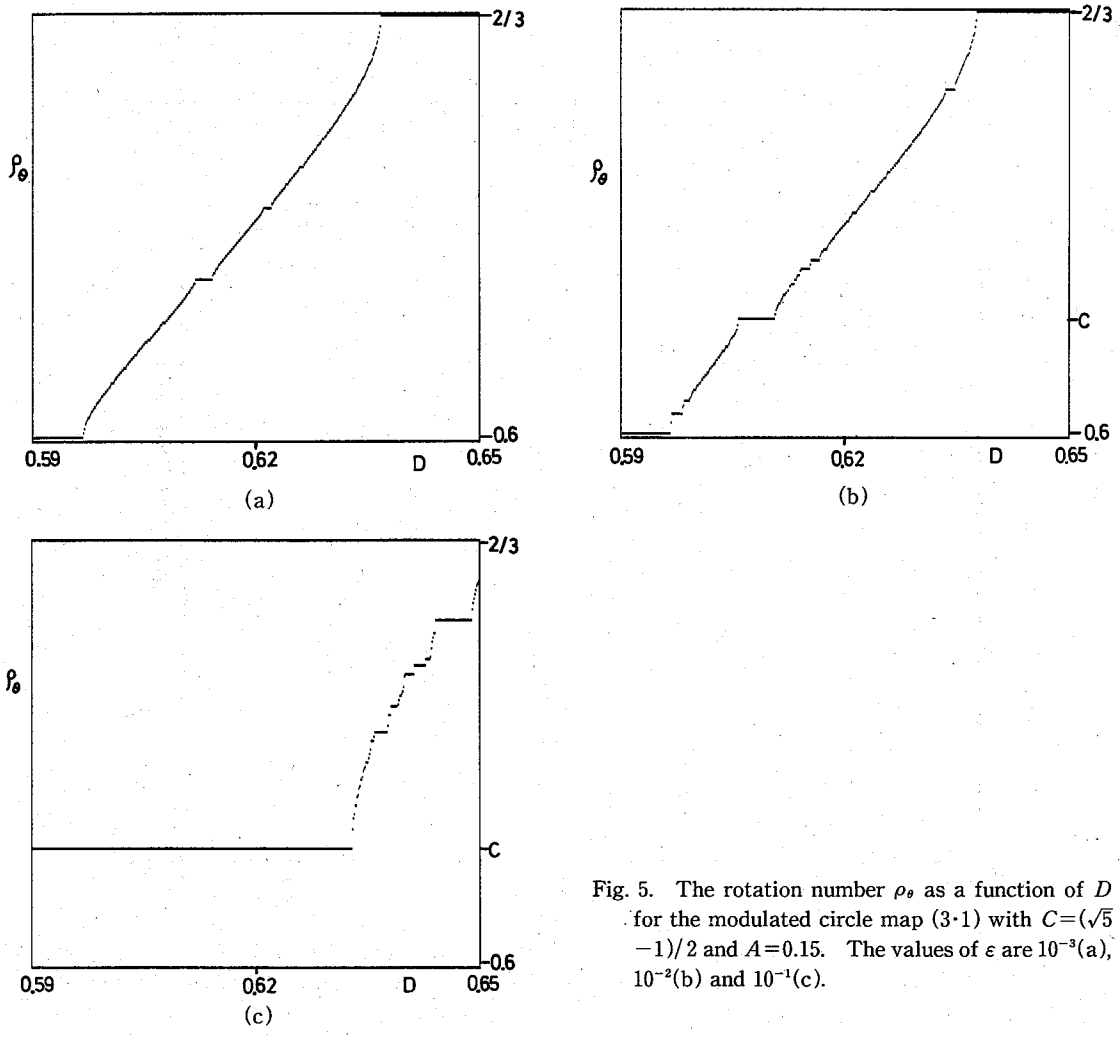

Fig. 5. The rotation number ρ_θ as a function of D for the modulated circle map (3·1) with $C=(\sqrt{5}-1)/2$ and $A=0.15$. The values of ε are 10^{-3}(a), 10^{-2}(b) and 10^{-1}(c).

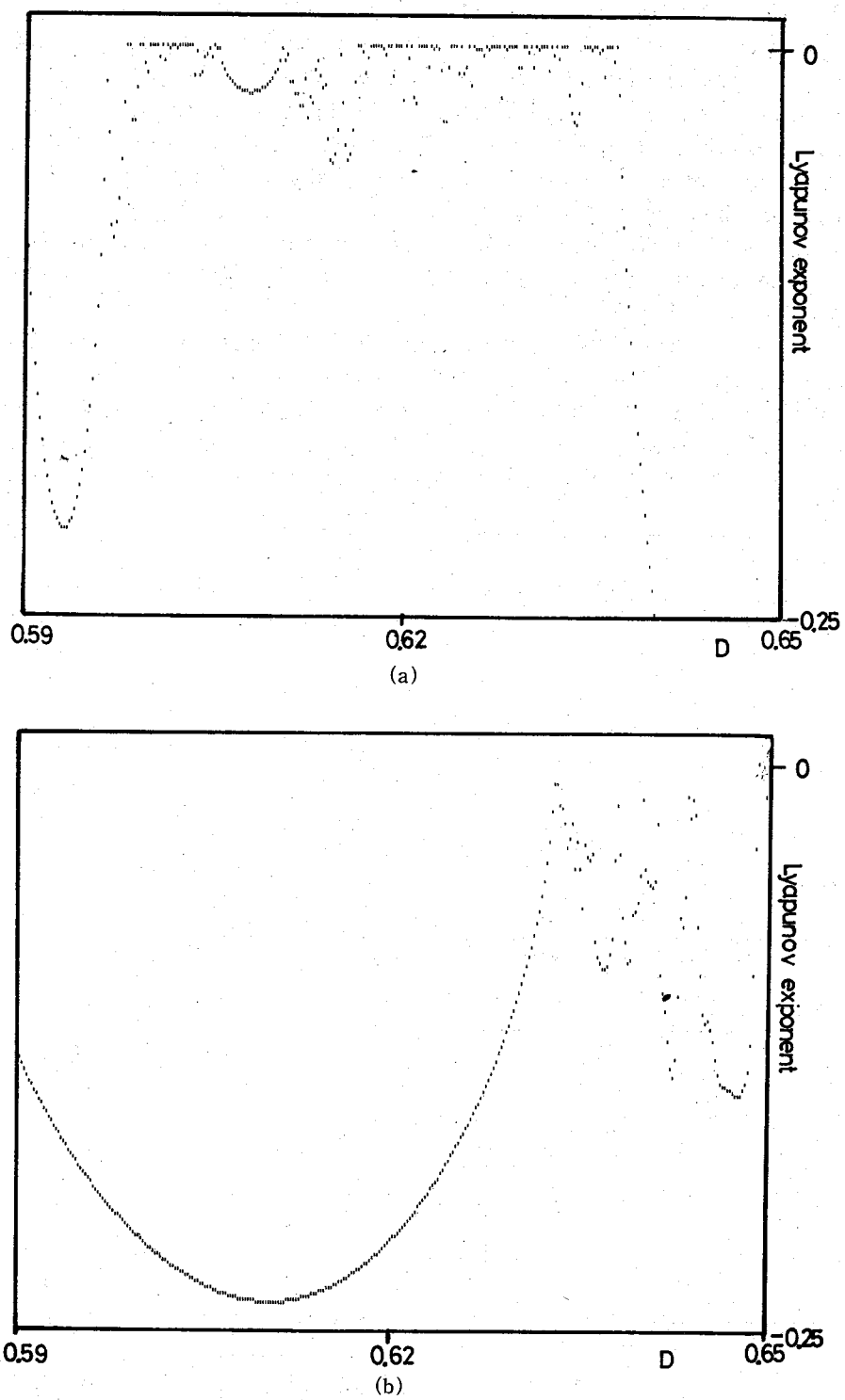

Fig. 6. The second Lyapunov exponent of the modulated circle map (3·1) with $C=(\sqrt{5}-1)/2$ and $A=0.15$, while the first Lyapunov exponent is always zero (trivial). It is plotted as a function of D for $\varepsilon=10^{-2}$(a) and $\varepsilon=10^{-1}$(b).

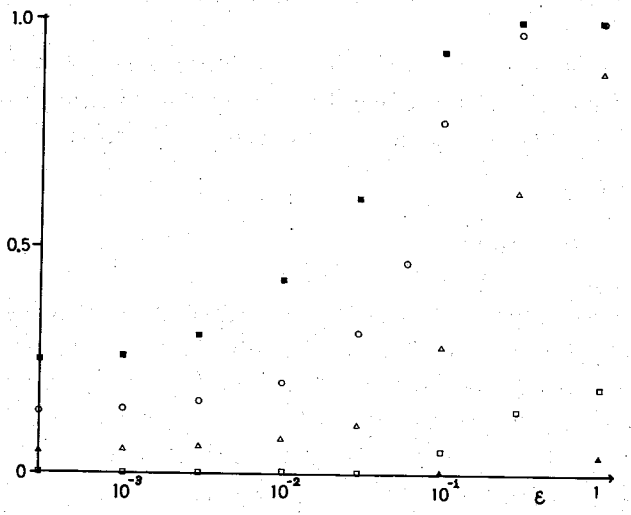

Fig. 7. The ratio of the locking (to torus) of the modulated circle map (3·1) with $C=(\sqrt{5}-1)/2$. We calculated the second Lyapunov exponent by 5×10^4 iterations and if the exponent is less than -10^{-4}, we regarded that the attractor is torus. We chose the value $D=D_i=0.55+0.0005i(0\leq i\leq 600)$ and calculated the ratio, defined by (the number of D_i at which the attractor is torus)/601, for given ε and A. The values of A are $0.9/(2\pi)$(■), $0.8/(2\pi)$(○), $0.6/(2\pi)$(△), $0.2/(2\pi)$(□), and $0.06/(2\pi)$(▲).

Table I, the region of the lockings with $\rho_\theta=q/p+Cs/r(s\neq0)$ increases as ε is increased, while the region of the locking with $s=0$(e.g., $\rho_\theta=2/3$) decreases. Since the number of elements to construct the staircase in Fig. 5 is two (i.e., C and 1), it may be called the "double devil's staircase". The second Lyapunov exponent as a function of D is given in Fig. 6(a) and (b).

As is seen in Figs. 5 and 6, the region of lockings increases as the coupling ε is increased. This is typically shown in Fig. 7, where the ratio of the locking region is plotted as a function of log ε. The above observation agrees well with the decrease of the region of three-torus due to the coupling, found in the simulations in §2.

In summary, the various features of a three-torus in §2 can be explained through the results of this section.

Before closing this section, we give some observations about the transition to chaos.

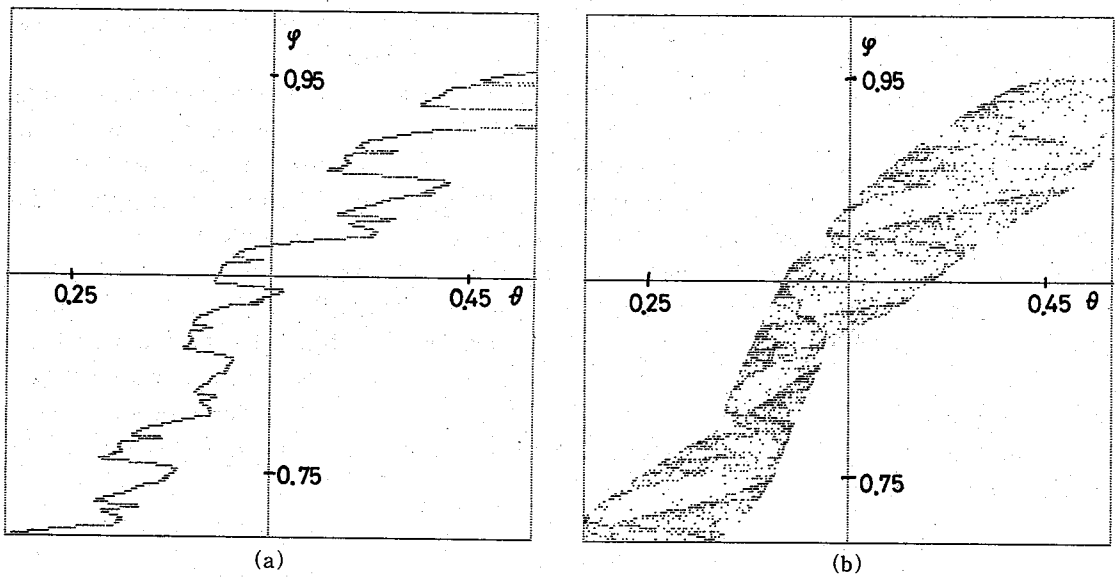

Fig. 8. The attractor of the modulated circle map (3·1) with $\varepsilon=0.05$, $D=0.615$ and $C=(\sqrt{5}-1)/2$. Only a part of the attractor is shown. The values of A are 0.178 (a) and 0.182 (b).

In Figs. 3(a), (b), the instability of the torus with $\rho_\theta = C$ and the transition to chaos are depicted.

The oscillation of torus is remarkably seen in Fig. 8(a). This type of the oscillation of torus is also observed in other two-dimensional mappings[7),15)] and in the doubling of torus.[13),15)] The oscillation is magnified as A is increased, which causes the transition to chaos.

§ 4. Discussion

In the present paper, we have investigated the fates of three-tori in dissipative mappings. There is a pioneering work on the structural instability on the three-torus by Ruelle and Takens.[1)] The structural stability however, is not necessary for the state to be physically observed. In our simulations, the three-torus is observed as the direct product state just like the torus. As the nonlinearity (or coupling) is increased, the region of three-torus decreases. Direct transition from a three-torus to chaos, however, is not observed. The transition to chaos occurs only via a locking into cycle from torus, which also is a locking from a three-torus. Taking into account the recent observation[12)] that the transition from torus to chaos occurs only via a locking, we may have a conjecture that the transition from n-torus to chaos occurs only via a cycle, which appears via a torus, which again appears via a three-torus, which again $\cdots$, $\cdots$, via an $(n-1)$-torus.

As the coupling is increased, the direct product state is destroyed and the three-torus completely vanishes and is locked into torus for various models, which may be a reason why the three-torus is not so frequently observed as the torus. We have to note that the appearance of strange attractor via the Hopf bifurcation of torus[1)] has never been observed in our simulations.

The locking into torus from three-torus forms a "double devil's staircase". As for the locking into cycle, a great effort has been performed to understand the devil's staircase.[3),6)] We do not have, however, any theory on the "double devil's staircase" , such as on the width of the locking or on the approach by a continued fraction or on the (in)completeness of the staircase. These problems are left to future studies.

The oscillation of torus, which is similar to the one observed in a delayed logistic map and is connected with the oscillation of an unstable manifold,[15)] is clearly seen at the transition to chaos in a modulated circle map. This behavior of the oscillation is essentially the same as the one observed in a doubling of torus[15)] and may be typical for the modulated maps, though the detailed mechanism of it is not yet clear.

In the present paper, the properties of chaos are not treated. Global properties of chaos after the collapse of tori, which are under investigation for a circle map,[11)] will be an important problem. As the nonlinearity is increased further, the second and third Lyapunov exponents take positive values, where the stability of a direct product state (chaos $\otimes$ chaos, etc) seems to be restored. This observation may be a useful step to understand the "fully-developed chaos"*) in terms of a direct product state of a low dimensional mapping.

*) We use this terminology in the sense that the chaos has a large number of positive Lyapunov exponents.

Acknowledgements

The author would like to thank Professor M. Suzuki for useful discussions and critical reading of the manuscript and thank Professor Y. Takahashi for useful discussions. He would also like to thank LICEPP for the facilities of FACOM M190. This study was partially financed by the Scientific Research Fund of the Ministry of Education, Science and Culture.

Appendix

In this appendix, the feature of a delayed map is given. We consider a delay differential equation[25)~28)]

$$\gamma^{-1}\dot{x}(t)=f(x(t-t_R))-x(t), \tag{A·1}$$

which is investigated in nonlinear optics,[25)] physiology[27)] and ecology[28)],etc. The K-point discretization of Eq. (A·1) gives a K-dimensional map,

$$x_{n+1}=\gamma f(x_{n-K+1})+(1-\gamma)x_n\,. \tag{A·2}$$

As a special case we consider the case $K=2$. The Jacobian of of this map is given by

$$\begin{pmatrix}1-\gamma & \gamma f'(x)\\ 1 & 0\end{pmatrix}, \tag{A·3}$$

the eigenvalues of which are $\{(1-\gamma)\pm\sqrt{(1-\gamma)^2+4\gamma f'(x)}\}/2$. Thus, the fixed point $x^*=f(x^*)$ loses its stability via a Hopf bifurcation as $f'(x^*)$ gets less than $-1/\gamma$ and a torus appears.

If we choose $f(x)$ as a logistic model, a delayed logistic map (2·1) is obtained (see Ref. 13) for 3- or 4- point delayed logistic model). For $A=0.4$, the Hopf bifurcation occurs at $D=D_c=3-2A=2.2$ and torus appears for $D>D_c$. The torus is collapsed and the chaos appears for $D\gtrsim 2.59$ via a locking into a cycle. The behavior and mechanism of the collapse is given in Refs. 7) and 15).

References

1) D. Ruelle and F. Takens, Commun. Math. Phys. **20** (1971), 167.
2) S. Newhouse, D. Ruelle and F. Takens, Commun. Math. Phys. **64** (1978), 35.
3) S. J. Shenker, Physica **5D** (1982), 405.
4) L. Glass and R. Perez, Phys. Rev. Lett. **48** (1982), 1772.
5) K. Kaneko, Prog. Theor. Phys. **68** (1982), 669.
6) K. Kaneko, Prog. Theor. Phys. **69** (1983) 403.
7) K. Kaneko, Prog. Theor. Phys. **69** (1983), 1427.
8) M. J. Feigenbaum, L. P. Kadanoff and S. J. Shenker, Physica **5D** (1982), 370.
9) S. Ostlund, D. Rand, J. Sethna and E. D. Siggia, Physica **8D** (1983), 303.
10) L. P. Kadanoff, J. Stat. Phys. **31** (1982), 1.
11) K. Kaneko, to appear in *Turbulence and Chaotic Phenomena in Fluids* ed. T. Tatsumi (North Holland).
12) L. H. Jensen, P. Bak and T. Bohr, Phys. Rev. Lett. **50** (1983), 1637.
13) K. Kaneko, Prog. Theor. Phys. **69** (1983), 1806.
14) A. Arnéodo, P. H. Coullet and E. A. Spiegel, Phys. Lett. **94A** (1983), 1.
15) K. Kaneko, "Oscillation and Doubling of Torus", to be published.
16) H. Daido, preprint.
17) V. Franceschini, preprint (to appear in Physica ***D***).

18) M. Sano and Y. Sawada, preprint.
19) J. P. Gollub and S. V. Benson, J. Fluid Mech. **100** (1980), 449.
20) A. Libchaber, S. Fauve and C. Laroche, Physica **7D** (1983), 73.
21) H. Yahata, Prog. Theor. Phys. **69** (1983), 396.
22) O. E. Rössler, Phys. Lett. **71A** (1979), 155.
23) I. Shimada and H. Nagashima, Prog. Theor. Phys. **61** (1979), 1605.
24) See, for example, Ref. 9).
25) K. Ikeda, H. Daido and O. Akimoto, Phys. Rev. Lett **45** (1980), 709.
26) J. D. Farmer, Physica **4D** (1982), 366.
27) M. C. Mackey and L. Glass, Science **197** (1977), 287.
28) R. May, Annals of NYAS **357** (1980), 267.

Notes added in proof : After the present paper was submitted, a letter by C. Grebogi, E. Ott and J. A. Yorke appeared in Phys. Rev. Lett. **51** (1983), 339, where the stability of 3-torus is also numerically investigated using the coupled circle map.

The oscillation of torus in modulated mappings (see Fig. 8) has recently been investigated in some detail and it is shown that the torus becomes fractal at the onset of chaos (K. Kaneko, to appear in *Chaos and Statistical Mechanics* (Springer; ed. Y. Kuramoto) and preprint (Oct. 1983); see also J. P. Sethna and E. D. Siggia, preprint).